Optical and Quantum Electronics (2020) 52:173
https://doi.org/10.1007/s11082-020-02284-x

Femtosecond laser surface engineering of biopolymer ceramic scaffolds coated with ZnO by low temperature atomic layer deposition method

L. Angelova[1] · I. Bliznakova[1] · A. Daskalova[1] · B. Blagoev[2] · A. Trifonov[3] · P. Terziyska[2] · I. Buchvarov[3]

Received: 17 October 2019 / Accepted: 21 February 2020 / Published online: 10 March 2020

Abstract
Surface femtosecond laser texturing of biopolymer and biopolymer/ceramic composites with subsequent ZnO film deposition on the samples by low temperature Atomic Layer Deposition (ALD) method was performed. In the current study, the deposition of ZnO layers was implemented at temperature 50 °C under pressure of 2 mbar. In order to investigate the effect of diverse ZnO thin films thickness, 100 or 500 repeating ALD cycles were applied. The samples were exposed to ultra-short laser pulses of 130 fs duration generated by a CPA (chirped pulse amplifier) Ti:Sapphire laser system. The artificial scaffolds were irradiated by varying the laser fluence (0.2 J/cm^2, 0.41 J/cm^2 and 2.07 J/cm^2) and the number of applied laser pulses (N = 1, 2, 5 and 10). The morphology and chemical properties of the treated samples were evaluated by Scanning Electronic Microscopy, Energy-Dispersive X-ray Spectroscopy and X-ray photoelectron spectroscopy. By combining fs laser modification with low temperature ALD method, essentially improved bioactivity properties of hybrid organic–inorganic bone tissue scaffolds could be achieved, which is of great importance for future tissue engineering application of the samples.

Keywords Biopolymer/ceramic composites · Femtosecond laser modification · Atomic layer deposition · Tissue engineering

This article is part of the Topical Collection on Advanced Photonics Meets Machine Learning.

Guest edited by Goran Gligoric, Jelena Radovanovic and Aleksandra Maluckov.

✉ L. Angelova
liliya_angelova@ie.bas.bg

[1] Institute of Electronics, Bulgarian Academy of Sciences, Sofia, Bulgaria

[2] Institute of Solid State Physics, Bulgarian Academy of Sciences, Sofia, Bulgaria

[3] Faculty of Physics, St. Kliment Ohridski University of Sofia, Sofia, Bulgaria

1 Introduction

Tissue engineering and regenerative medicine have become the standard field for replacing organ and tissue loss or failure, resulting from injury and other types of damage, which happen to be major human health problems. In fact, not quite long ago, the use of bone tissue or organ transplantation was severely limited by donor shortage (Olson et al. 2011). Current use of drug therapy, surgical reconstruction and medical devices are always available, but they tend to exhibit problems, such as incapability of replacing all the functions of the damaged or lost bone tissue. Among the recent technologies in the multidisciplinary field of tissue engineering or regenerative medicine, use of various types of scaffolds is the key component (Olson et al. 2011; Pighinelli et al. 2016). Scaffolds are the best materials for restoring, maintaining and improving tissue function. They play a unique role in repair and more importantly regeneration of bone tissues by providing a suitable platform, permitting essential supply of various factors associated with survival, adhesion, proliferation and differentiation of cells (Scheinpflug et al. 2018; Alaribe et al. 2016). Scaffolds could be made of synthetic or absorbable, naturally occurring, biological, degradable or non-degradable polymeric and/or ceramic materials. These scaffolds act as a support structure for the cell attachment and growth into tissues and must have adequate mechanical and anti-inflammatory properties (Dahlan et al. 2012; Mukherjee 2014; Derakhshanfar et al. 2018; Wua et al. 2014). Hydroxyapatite (HAp) is a mineral naturally found in bones and is used for fabrication of dense and porous bioceramics (Wua et al. 2014; Gervaso et al. 2012) as it increases the osteoconductive bonding of implants with surrounding tissues (Milella et al. 2001). Zirconia (ZrO_2) has excellent chemical and dimensional stability and mechanical strength (Tosiriwatanapong and Singhatanadgit 2018). Its anti-inflammatory qualities are well known and make it a desirable component in hybrid bone and dental matrixes (Nevins et al. 2011; Kohal et al. 2013). Apart from its biomedical significance (Zhu et al. 2016; Laurenti and Cauda 2017), ZnO thin films (Laurenti et al. 2015), nanowires (Cui 2012), nanorods (Li et al. 2001), nanoparticles (Dumontel et al. 2017), etc., find broad application in a huge number of practical areas (Ozgur et al. 2005). These include surface acoustic wave sensors (Fu et al. 2010), gas sensors (Wang et al. 2010; Eranna et al. 2004), energy harvesting systems (Wang and Song 2006), perovskite solar cells (Li et al. 2017; Wang et al. 2019; Zang 2018), light-emitting diodes (Zang et al. 2016), thin-film based transistors (Fortunato et al. 2012), photodetectors (Soci et al. 2007), semiconductors (Janotti and Van de Walle 2009), etc. Chitosan (Ch) is a natural biopolymer with high biocompatibility, antimicrobial activity and superior affinity to proteins (Arca and Senel 2008; Martino et al. 2005).

It is recognized that the behavior of the cell adhesion, proliferation, and differentiation on materials depends largely on surface characteristics such as wettability, chemistry, charge, rigidity, and roughness (Saito et al. 2015). Femtosecond laser-assisted method for surface processing is a promising method since it is non-contact, with high degree of reproducibility, does not require chemical agents, it can create various nano- and microstructures with increased roughness. Laser processing allows the fabrication of precise well-defined patterns, which makes it very attractive for tissue engineering applications (Narayan et al. 2007; Terakawa 2018). By employing femtosecond laser radiation, the mechanical properties of the engineered scaffolds remain unchanged after the laser treatment (Mukherjee 2014; Govindarajan and Shandas 2014).

Atomic layer deposition (ALD) is a type of chemical vapor deposition, with precursor delivery in a sequential manner. Separation of precursors in time leads to self-limiting

surface reactions, which result in layer by layer deposition. That leads to conformal and uniform covering with 3D structures with high- surface to volume ratio and accurate control of the thickness on a nanometer scale. Narayan et al. (2010) suggested that ALD is an appropriate method for nanoporous alumina functionalization. Their claims were once again confirmed by Cuevas et al. (2019), who analyzed optical and chemical changes of nanoporous alumina structure, coated with different metal oxides and nanolayers by ALD and demonstrated that ALD is an attractive method for further biomedical applications of alumina substrates. Low temperature process allows film deposition on biomaterials without their degradation. As an addition to that, low temperature ALD of ZnO provides high antibacterial efficiency of the surface processed (Johnson et al. 2014; Oviroh et al. 2019).

In this study both surface modification methods described above were applied on biopolymer ceramic composites based on Ch and Ch/HAp/ZrO_2, in order to monitor their complementary impact on the scaffolds properties for optimizing their application in bone tissue engineering. A few studies have reported functionalization of chitosan by mixing it with ceramic materials. For example, Wang and Yeung (2017) and Muzzarelli (2011), reviewed in detail, diverse approaches for applying polymer coatings or creating polymer-bioceramic microstructures that imitate the composite arrangement of bone and could be applied for bone regeneration.

The current challenge is related to creation of 'smart' biomimetic scaffolds by combining the two described techniques to induce enhanced surface functionalization by tailoring topographic surface modification.

Surfaces are the primary place of contact between a biomaterial and its host organism. By tailoring the material surface morphology, functionalization of the biomaterials can be achieved, by enhancing its biocompatibility and promoting cells integration, which is the future task of this primary experiments. In order to obtain valuable information for optimising the treated samples, their morphology and chemical properties were evaluated by SEM, EDX, and XPS analyses.

2 Materials and methods

For the purposes of the investigation, samples of chitosan (Sigma—Aldrich®, medium molecular weight) and Ch/HAp/ZrO_2 composites in different percent correlation (w/v) were prepared in the form of thin films on glass substrates. The protocol of their preparation is presented elsewhere (Daskalova et al. 2019) (Fig. 1a). Femtosecond laser modification was applied in order to obtain a microporous structure on the sample surface (Fig. 1a). In the experiments, an amplified Ti:Sapphire laser system (Quantronix- Integra-C) emitting at central wavelength $\lambda = 790$ nm, 130 fs pulse duration and 1 kHz repetition rate was used. In order to optimize the samples texturing, the laser fluence (0.2–2.07 J/cm^2), and the number of applied laser pulses (N = 1–10), were varied. The thin films were modified with a pattern of parallel stripes by the femtosecond Ti:sapphire laser, described in (Daskalova et al. 2019). The laser beam was focused with a lens with focal length of 200 mm. The focal spot diameter was estimated to be 40 μm. The laser patterning was performed by scanning the laser beam across the samples surfaces in the X direction to produce a stripe-like modification. The sample was positioned on a motorized XYZ translation stage. The experiment was performed in air. The scanning velocity was set to 2.5 mm/s creation of the rows. The whole setup was controlled by a Labview software. In this way, the non-contact laser texturing of the samples leaded to morphological modification of the surface, without

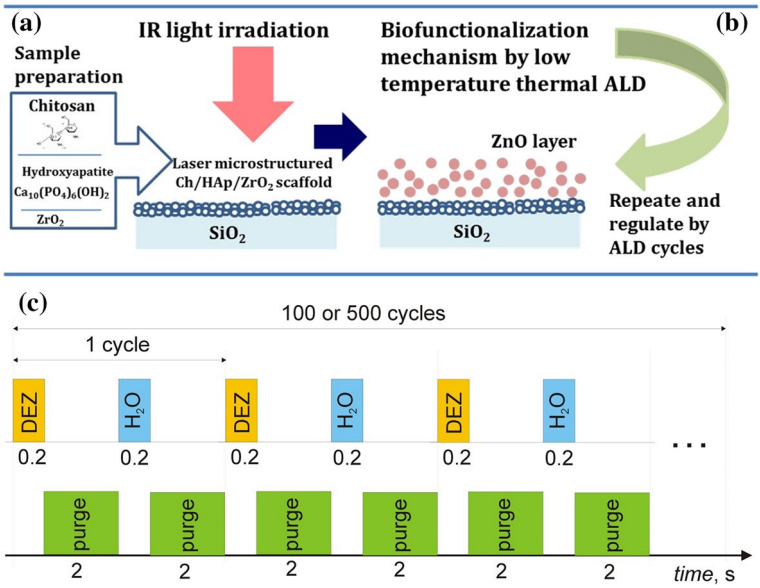

Fig. 1 Schematic illustration of the main experimental steps: **a** femtosecond microstructuring of the prepared biopolymer/ceramic scaffolds; **b** ZnO coating by ALD method of the samples **c** mechanism of ALD DEZ-H_2O step, repeated 100 or 500 times, respectively

compromising the biochemical structure of the composite sample. As a result, porous texturing and higher surface to volume ratio were obtained. Surface topography of the biomaterials affects the ability of cell adhesion and interaction, which is critical to achieving optimal bioactivity. Control over nanostructures can be especially powerful in controlling cell behavior. The cells react strongly on the surfaces; they adhere, distribute and change their shape according to the geometry of the matrices (Ma 2001). After laser treatment, the processed samples were coated with thin ZnO film deposited by low temperature atomic layer deposition (ALD) (Fig. 1b). Thin ZnO films were prepared in a Beneq TFS-200 ALD reactor on several groups of biopolymer substrates and on referent n-Si (100) substrate. The deposition process was conducted at temperature 50 °C under pressure of 2 mbar. To obtain ZnO films alternating diethyl zinc $(C_2H_5)_2Zn$ (DEZ) as a zinc precursor and deionized water (H_2O) as an oxygen precursor were used (Fig. 1c). Each precursor pulse was followed by pure Nitrogen (N_2) purging pulse. The pulse and purging durations were the same for the both precursors—200 ms and 2 s, respectively. A pure N_2 gas flow at 300 sccm was maintained in the reaction chamber during the deposition process. Hundred (100) and five hundred (500) ALD cycles were applied on the created microstructures in order to investigate the effect of different layer thickness. By varying the number of cycles, high precision and uniform growth of ZnO on the complex substrates is possible. ALD is a deposition method with great potential for producing very thin, 3D—conformal films with control of the thickness and ZnO attachment at atomic level. The surface roughness, achieved because of fs processing, is assumed to be one of the key factors for optimized coating of the samples with ZnO thin layers, and additional conformational change of their surface. Such combined modification of bone tissue scaffolds can essentially improve bioactivity properties of hybrid organic–inorganic biomaterial.

The morphological change of the synthesized biopolymer and biopolymer/ceramic thin layers was examined by a Scanning Electron Microscope (SEM analysis, SEM-TESCAN/LYRA/XMU). Energy Dispersive X-ray spectroscopy (EDX) was performed for identifying and quantifying elemental compositions of the examined thin films. Each spectrum was measured with operating voltage of 20 kV before and after femtosecond laser irradiation was conducted. X-ray photoelectron spectroscopy (XPS) was done by means of an AXIS Supra electron spectrometer (Kratos Analytical Ltd., Manchester, UK). Chemical analysis of the samples of interest (unprocessed and laser processed) with high-resolution were obtained, as the variation of the applied laser fluence and pulses have been taken into account. In order to investigate biomedical application of laser-induced surface texturing of tissue scaffolds coated with ZnO by thermal ALD method, several techniques were used.

3 Results and discussion

3.1 Morphology and elemental analysis of ZnO coated microporous scaffolds

SEM images revealed the morphology of the obtained structures of Ch-ZnO(100) and Ch/1%HAp/1%ZrO_2–ZnO(100) before and after laser irradiation (Fig. 2).

The structures formed after laser texturing and ALD coating of biopolymer thin film (Fig. 2b, c) have foam-like appearance, while the composite sample (Fig. 2e, f) possess groove shape which results in different roughness on the material surface. The main reason for the difference in the observed morphological structures originates from variations in the thin film layer composition, applied laser parameters and scanning modes. The deposition of ZnO layer over the biopolymer/composite blends was estimated by comparison of Energy-Dispersive X-ray Spectroscopy (EDX) analysis for laser processed and non-processed regions of the samples. The obtained results demonstrate improved attachment of the zinc oxide over the laser textured areas compared to the non-treated ones (Fig. 3).

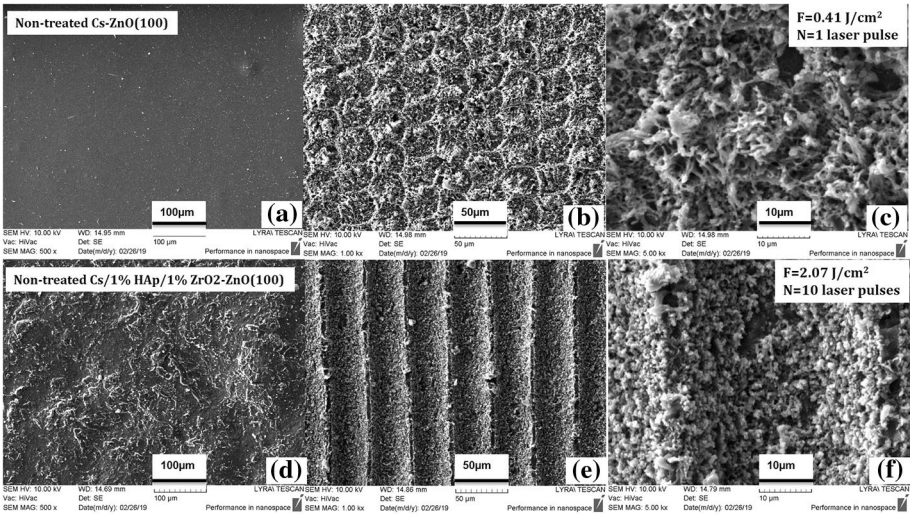

Fig. 2 SEM images of the artificial scaffolds: **a–c** Ch–ZnO(100) and Ch/HAp/1%ZrO_2–ZnO(100) **d–f** Femtosecond processed Ch–ZnO(100)-**b**, **c** and Ch/1%HAp/1%ZrO_2–ZnO(100)-**e**, **f**

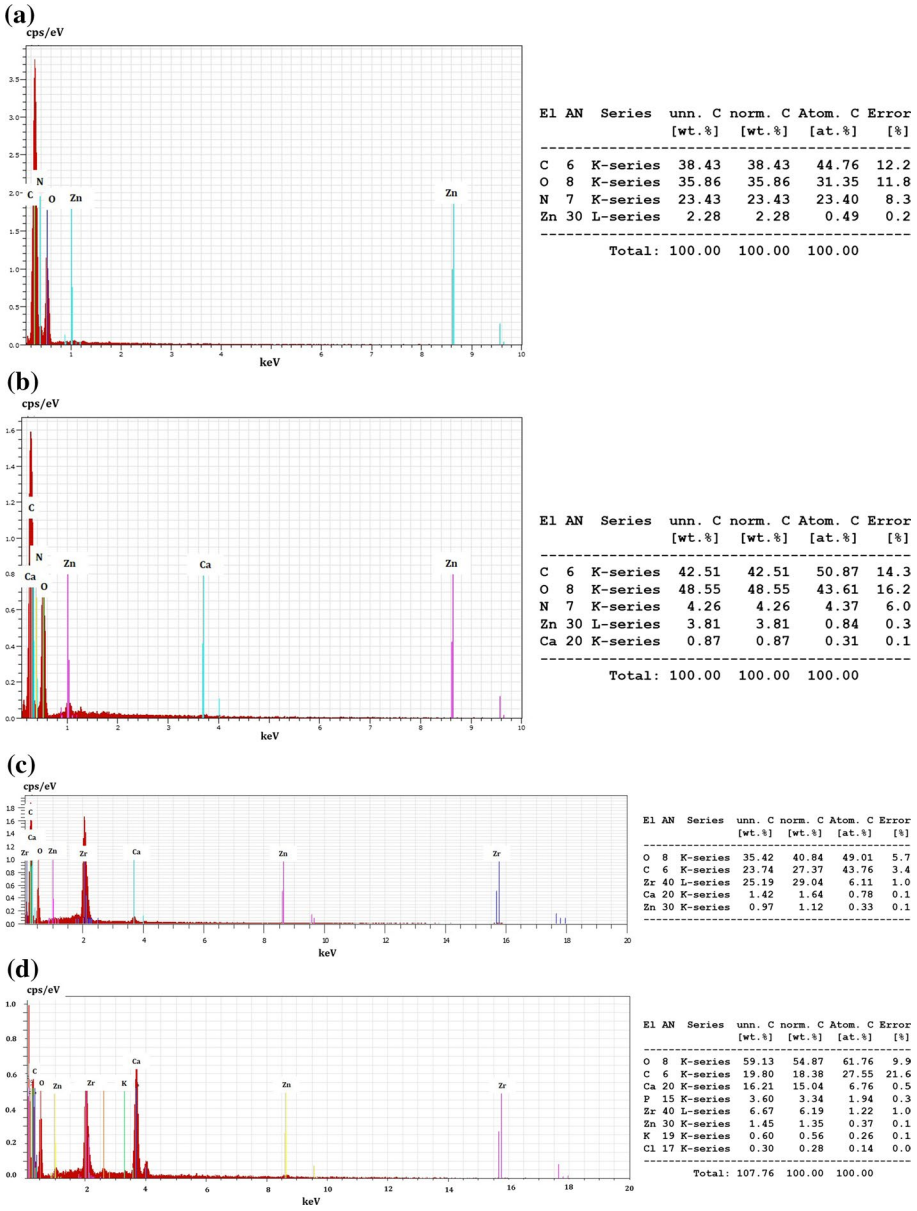

Fig. 3 Energy-Dispersive X-ray Spectroscopy (EDX) analysis of: **a** non-treated Ch–ZnO(100) **c** Ch/1%HAp/1%ZrO_2–ZnO(100); laser treated areas of **b** Ch-ZnO(100) and **d** Ch/1%HAp/1% ZrO_2–ZnO(100)

EDX analysis represents the atomic percentages of the elements of interests C, O, N, Zn and Ca for each region. From the acquired results could be concluded that the ZnO attachment over the laser textured zones of the biopolymer and composite scaffolds increases in comparison to unmodified ones. This is confirmed by the weight percent values of the

elements detected Fig. 3 (right)—Zn (wt%) increases from 2.28 to 3.77 for Ch–ZnO(100) and from 0.97 to 1.45 for Ch/1%HAp/1%ZrO_2–ZnO(100). Laser treatment leads to deviation in the surface roughness (Daskalova et al. 2019), which in turns triggers better ZnO deposition on the modified layers, due to increased surface area.

3.2 Chemical analysis of examined thin films

X-ray photoelectron spectroscopy (XPS) was performed to evaluate the presence of ZnO deposition on the surface of the samples and to compare the number of applied growth cycles on the Ch-ZnO(500) samples (Fig. 4). Analysis is performed also for the compositions of 70%Ch30%HAp/1%ZrO_2–ZnO(100) and Ch/1%HAp/1%ZrO_2–ZnO(500) layers (Fig. 5). All recorded spectra are related to the non-treated areas on the scaffold to serve as control (the lowest row of both figures) and visualize the characteristic differences. High-resolution detailed scans were performed around peaks of interest C_{1s}, Ca_{2p}, Ca_{2s}, N_{1s}, O_{1s}, Zn_{2p}, Si_{2p}, and Zr_{3d} (Figs. 4 and 5). The samples of Ch-ZnO(500) were processed with laser fluence of F = 0.41 J/cm^2, N = 1, 2 and 5 laser pulses (Fig. 4, rows 1,2 and 3, respectively;), and repetition rate ν = 50 Hz (Fig. 4a–h) and ν = 500 Hz (i–p). Curves are presented with different colors, according to number of fs pulses/non-treated surface on each row of the figure.

The first two spectra (Fig. 4a, b) present the region of C_{1s} peak, which is decomposed into several peaks, attributed to bonding energies of 284.8, 285.8, 286.3, 286.8, 288.0, and 289.0 eV corresponding to C–C/C–H bond and C–NH/C–NH_2 (Gao et al. 2009). The additional peak (Fig. 4b, orange) at the highest binding energy of 288.5-289.0 eV, as an exception to the ideal chitosan structure, is observed in all cases of laser treated samples, but not in the case of the non-treated areas of the scaffold. According to the theoretical considerations this peak can be attributed to C_{1s} binding energy of other carbon atoms. The results, presented at Fig. 4 are in agreement with the fundamental study of Jiang et al. (1997), as well as with the theoretical and experimental results, presented in the elaborate work of Kostov et al. (2018). Other regions of interest are the detected Ca_{2p} peak (Fig. 4c) decomposed to two peaks with corresponding energies: 344.59 and 348.25 eV (control surface); N = 1—at 345.30, 348.66 eV; N = 2—at 345. 10, 348.86 eV and N = 5—at 345.20, 348.86 eV. For Ca_{2s} (Fig. 4d) there is no detectable energy maximum for control surface and pronounced peaks are observed for N = 1,2 and 5 at 436.82, 436.99, and 437.15 eV, respectively. Another intense peak, appearing at 529.68 eV, could be assigned to hydroxyl groups ($-OH^-$) of O_{1S} line (Fig. 4f) (Kostov et al. 2018). A small amount of silicium (Si) was reported (Fig. 4h), and in the case of N = 5 it's quantity is increasing, which may be attributed to the fact that in this case the glass substrate of the sample is reached, due to the larger amount of material ablated by fs pulses. The Zn registration is by ZnO applied by the ALD method (Fig. 4g). In the case of repetition rate ν = 500 Hz Fig. 4i–p, no difference was observed in the energy peaks of C_{1s} (Fig. 4i), Zn_{2p} (Fig. 4m) and O_{1s} (Fig. 4o) for the non-treated and laser treated chitosan with N = 1. No detectable energy maximums were captured for the Ca_{2p} and Ca_{2s} (Fig. 4j, k), N_{1s} (Fig. 4l) and Zr_{3d} (Fig. 4p) for the control and fs treated chitosan surface, which confirms that these elements are not presented in the Ch-ZnO(500) sample.

On Fig. 5 comparison between the XPS spectra of C_{1s}, Ca_{2p}, Ca_{2s}, N_{1s}, Si_{2p} and Zn_{2p} regions are presented for Ch/1%HAp/1%ZrO_2–ZnO(500) (a–h) and 70%Ch30%HAp/1%ZrO_2–ZnO(100) (i–p) samples. The composites were treated with F = 2.07 J/cm^2 and N = 10 (upper row, in purple). As a control, laser non-treated sample

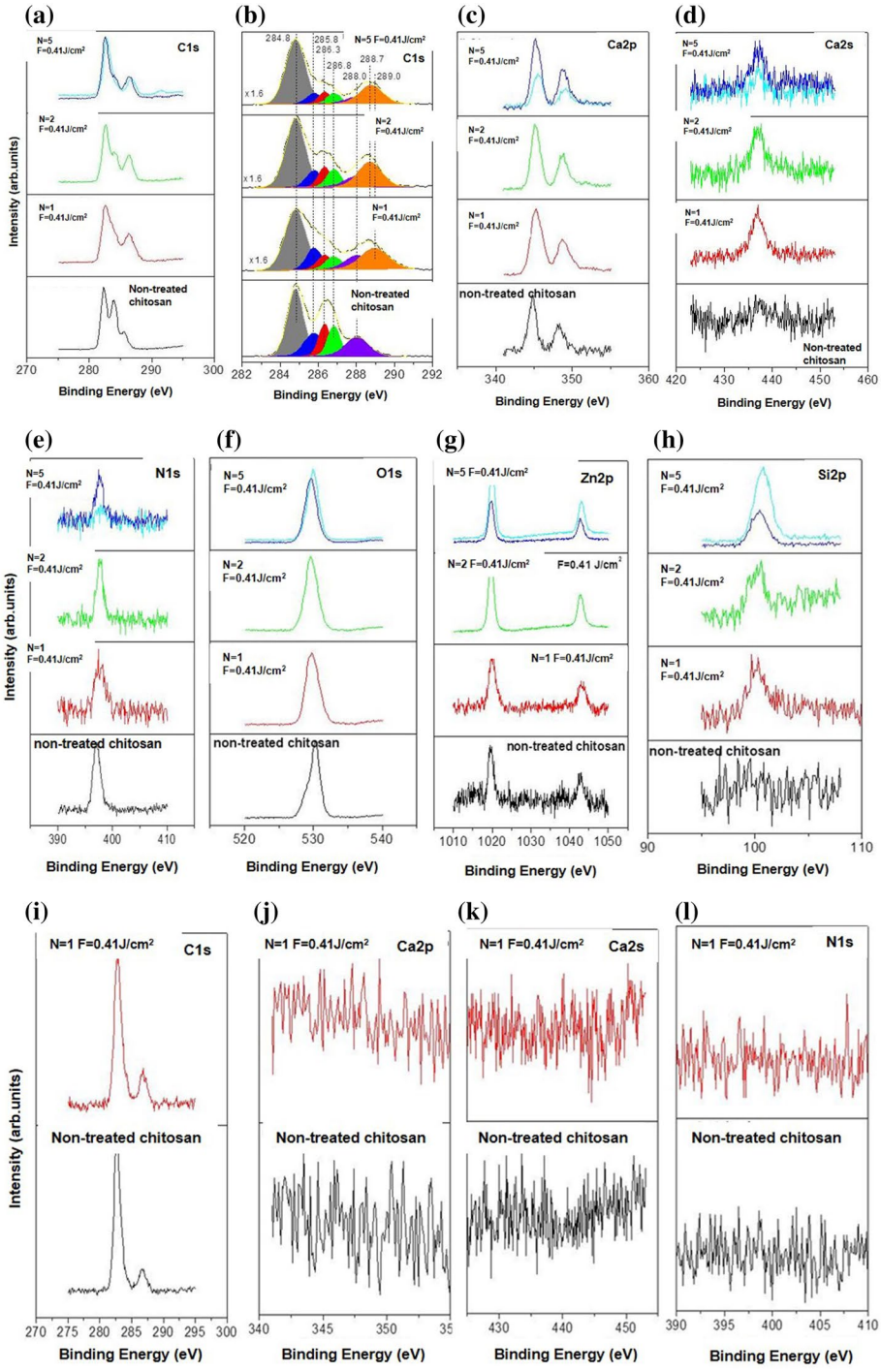

Fig. 4 X-ray photoelectron spectroscopy (XPS) detailed spectra of Ch–ZnO(500)

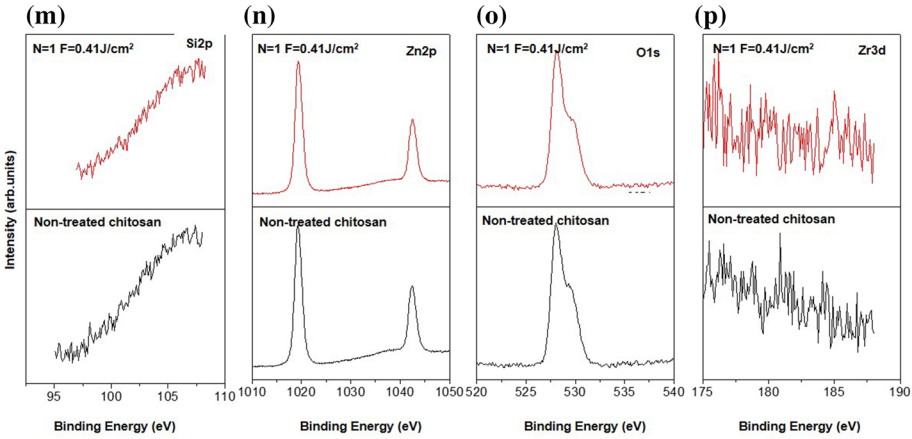

Fig. 4 (continued)

surface was used (lower row, in green). The typical structure of chitosan for the sample composition − 70%Ch30%HAp/1%ZrO_2–ZnO(100) is analogical to Fig. 4 and is clearly observed (Fig. 5i, j). This could be explained with the applied lower number of ALD cycles and the poor coverage of the laying underneath Ch-ceramic layer. In contrast, in the spectrum obtained from Ch/1%HAp/1%ZrO_2–ZnO(500) sample, the characteristic decomposition is absent (Fig. 5a). Similarly to the Ca peak (Fig. 5b, c), the detection of Zr on the spectrum from Ch/1%HAp/1%ZrO_2–ZnO(500) is not pronounced (Fig. 5e), in relation to the spectrum obtained for the sample with the composition 70%Ch30%HAp/1%ZrO_2–ZnO(100) (Fig. 5m), where Zr is detectable under the thinner layer of ZnO(100). The Zr element in the Ch/1%HAp/1%ZrO_2–ZnO(500) sample volume is not captured (Fig. 5e), due to the well covered ZnO layer on the top of the surface, as the XPS analysis is performed at average depth of 5 nm, which is less than the ZnO layer thickness (given afterwards).

The signal intensity of Zn peak is much higher in the case of a laser-treated surface (Fig. 5h, p). The results show a preferential adhesion of ZnO to the laser-processed sample surface. Supplementary evidence is the presence of peaks corresponding to chitosan structure underneath ZnO (100) layer, which is not observed in the case of 500 ALD cycles (Fig. 5h–o). Atomic percentages of the elements of interest are given in Table 1.

The results clearly demonstrate increment of atomic concentrations of both zinc and oxygen for all laser treated surfaces, as the number of laser pulses rises up. However, a slight deviation of Zn atomic concentration is observed for the case of Ch-ZnO(500), N = 2 and 5 pulses (5.9 and 3.9 at. conc. %, respectively). Considering the information given in Table 1, repetition of these preliminary measurements in subsequent experiments is planned in order to estimate the trend of the obtained data.

Results of the performed measurements with a Woollam M2000D rotating compensator spectroscopic ellipsometer (wavelength range from 193 to 1000 nm), show that the estimation of ZnO layer thickness is 38.0 and 13.1 nm for ZnO(500)- and ZnO(100)- biopolymer and biopolymer/ceramic samples, respectively. These thicknesses partly explains the XPS results, presented on Fig. 5, as analysis is performed at average depth of 5 nm. The data acquisition and analysis was obtained by CompleteEASE 5.10 J.A.Woollam Co., Inc software. The thicknesses of the ZnO layers were determined using spectroscopic ellipsometry

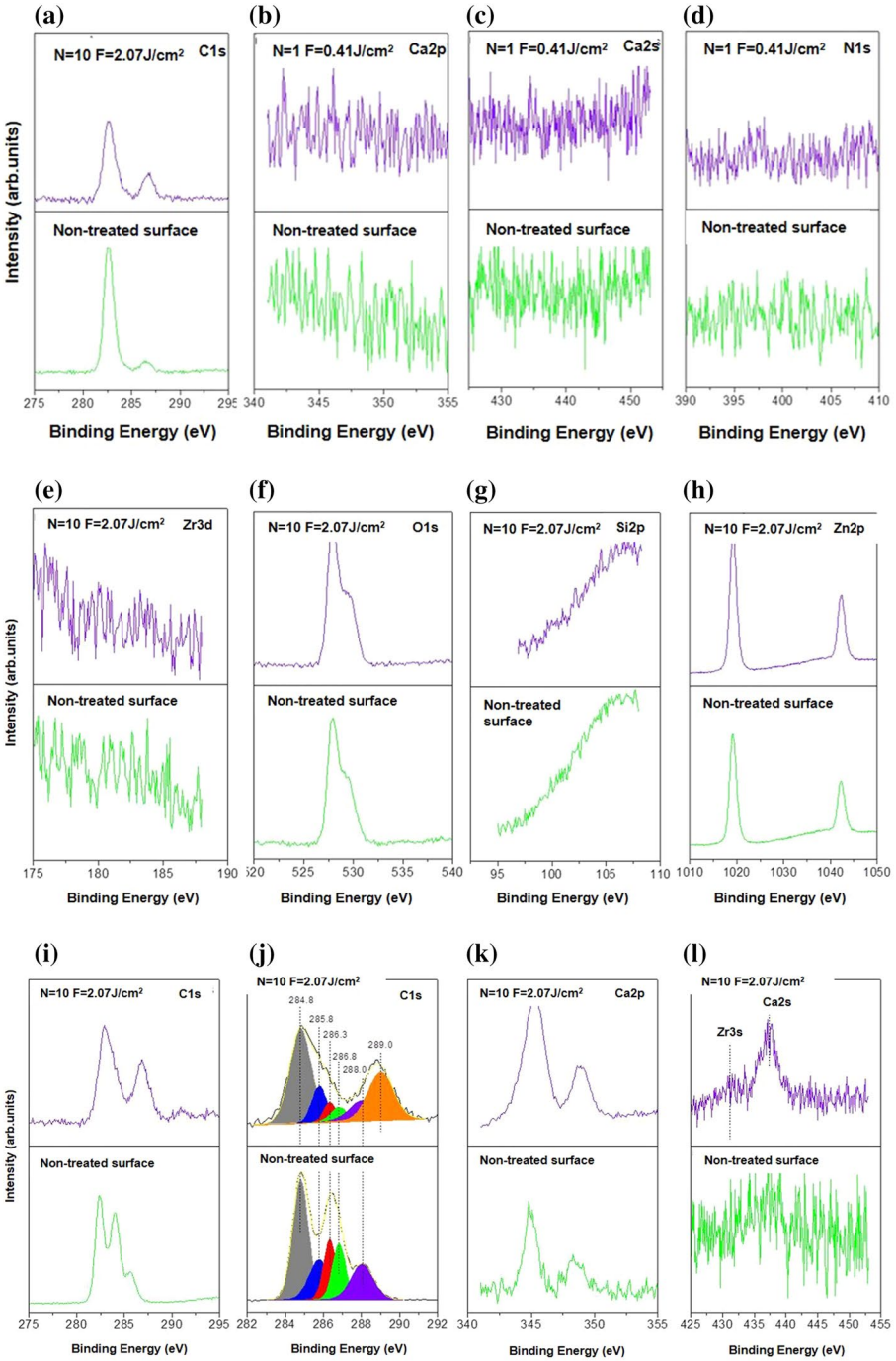

Fig. 5 Comparison between the XPS spectra of Ch/1%HAp/1%ZrO_2–ZnO(500) (**a**–**h**) and 70%Ch30%HAp/1%ZrO_2–ZnO(100) (**i**–**p**)

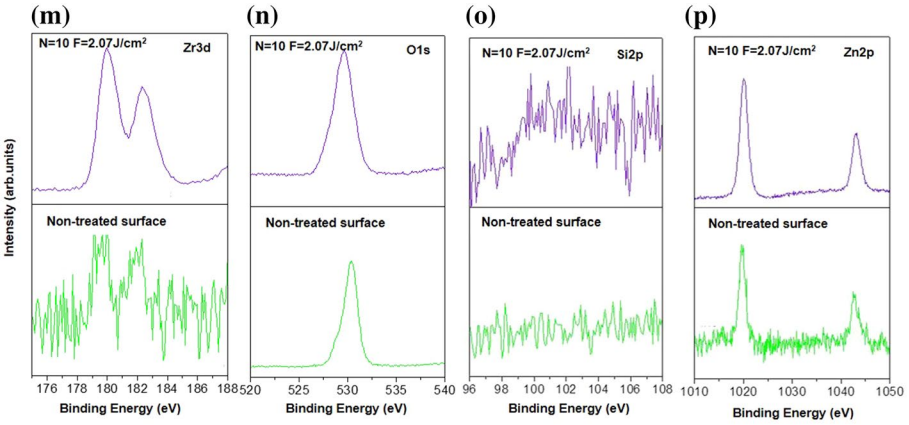

Fig. 5 (continued)

Table 1 Atomic concentration of XPS analysis

Sample	Zn at. conc. (%)	O at. conc. (%)	Zr conc. (%)
Ch-ZnO (500) non-treated surface	0.2	23.5	–
F = 0.41 J/cm^2, N = 1	0.7	32.4	–
F = 0.41 J/cm^2, N = 2	5.9	33.9	–
F = 0.41 J/cm^2, N = 5	3.9	37.0	–
70%Ch30%HAp/1%ZrO_2·ZnO (100) non-treated surface	0.5	23.8	0.1
F = 2.07 J/cm^2, N = 10	7.9	43.7	4.0

measurements of ZnO layers, deposited on accompanying Si substrates. The spectroscopic ellipsometry data Ψ and Δ (taken at angles of incidence of 50°, 60° and 70°) were analyzed using a three-layer model consisting of a silicon substrate with a 2.33 nm thick SiO_2 native oxide as a first layer, a ZnO as a second layer and a roughness layer as a third one. The interfaces between the different layers were assumed to be abrupt and the layers—homogeneous in depth. The optical constants of the ZnO layer were assumed to be isotropic. Tabulated values for the optical constants of the silicon substrate and the silicon native oxide from the CompleteEASE software database were used. The ZnO layers were represented by the general oscillator model consisting of one PSemi-M0 and one Gaussian oscillators. The roughness layer for all samples was modeled by Bruggeman's EMA (Effective Medium Approximation) of 50% voids and 50% bulk material (CompleteEASE® Software Manual (Lincoln: J.A.Woollam Co.) USA).

4 Conclusion

Experimental results obtained by the combination of femtosecond laser—induced surface modification of scaffolds with subsequent deposition of ZnO film by low temperature ALD method are presented. The samples were divided by the number of applied ALD

cycles-ZnO(100) and ZnO(500) cycles.The acquired data demonstrate significant efficiency of ZnO adhesion over the laser-treated surface in contrast to untreated one. These studies show that the ZnO(500) layer for all types of thin films seem to have improved attachment on the laser treated parts of the samples in comparison to ZnO(100). ALD process is based on surface chemical (adsorption) reactions and strongly depends on free chemical bonds on the surface. Laser treatment is producing micro-/nano- porous structure, which expands the surface of the sample. Furthermore, during laser treatment new chemical bonds are activated which facilitate ALD surface reactions. Because of the porous structure and the larger surface, the precursor did not penetrate into the pores. Repeating the ALD cycle many times drastically improves the attachment of ZnO on the surface. To clarify that, additional experiments with longer pulse durations should be implemented. The atomic percentage of elements of interest was evaluated by EDX and XPS analyzes. The obtained results clearly demonstrate that the combined application of ultra-fast laser treatment and low temperature ALD method for surface functionalization of biopolymer and biopolymer/ceramic composite materials leads to improved deposition of ZnO over laser-processed areas.

Acknowledgements This work was financially supported by the Bulgarian National Science Fund (NSF) under Project no. DM18/6 -"Ultra-short laser surface modification and property analysis of synthesized ceramic scaffolds used for bone tissue engineering" (2017–2019) and Project no. DN08/5 -"Bioactivity improvement of biomimetic materials by texturing with ultrashort laser pulses" (2016–2019).

References

Alaribe, F.N., Manoto, S.L., Motaung, ShCKM: Scaffolds from biomaterials: advantages and limitations in bone and tissue engineering. Biologia **71**, 353–366 (2016)

Arca, H., Şenel, S.: Chitosan based systems for tissue engineering part 1: hard tissues. FABAD J. Pharm. Sci. **33**, 35–49 (2008)

Cuevas, A., Martínez de Yuso, M., Vega, V., González, A., Prida, V., Benavente, J.: Influence of ALD coating layers on the opticalproperties of nanoporous alumina-based structures. Coat **9**, 43 (2019)

Cui, J.B.: Zinc oxide nanowires. Mater. Charact. **64**, 43–52 (2012)

Dahlan, K., Dewi, S., Nurlaila, A., Soejoko, D.: Synthesis and characterization of calcium phosphate/chitosan composites. Int. J. Bas. Appl. Sci. **12**, 50–57 (2012)

Daskalova, A., Bliznakova, I., Angelova, L., Trifonov, A., Declercq, H., Buchvarov, I.: Femtosecond laser fabrication of engineered functional surfaces based on biodegradable polymer and biopolymer/ceramic composite thin films. Polymers **11**(2), 378 (2019)

Derakhshanfar, S., Mbeleck, R., Xu, K., Zhang, X., Zhong, W., Malcolm Xing, M.: 3D bioprinting for biomedical devices and tissue engineering: a review of recent trends and advances. Bioact. Mat. **3**, 144–156 (2018)

Dumontel, B., Canta, M., Engelke, H., Chiodoni, A., Racca, L., Ancona, A., Limongi, T., Canavese, G., Cauda, V.: Enhanced biostability and cellular uptake of zinc oxide nanocrystals shielded with a phospholipid bilayer. J. Mater. Chem. B **5**, 8799–8813 (2017)

Eranna, G., Joshi, B.C., Runthala, D.P., Gupta, R.P.: Oxide materials for development of integrated gas sensors-a comprehensive review. Crit. Rev. Solid State Mater. Sci. **29**, 111–188 (2004)

Fortunato, E., Barquinha, P., Martins, R.: Oxide semiconductor thin-film transistors: a review of recent advances. Adv. Mater. **24**, 2945–2986 (2012)

Fu, Y.Q., Luo, J.K., Du, X.Y., Flewitt, A.J., Li, Y., Markx, G.H., Walton, A.J., Milne, W.I.: Recent developments on ZnO films for acoustic wave based bio-sensing and microfluidic applications: a review. Sens. Actuators B Chem. **143**, 606–619 (2010)

Gao, Y.K., Traeger, F., Shekhah, O., Idriss, H., Woell, C.: Probing the interaction of the amino acid alanine with the surface of ZnO (1010). J. Coll. Interface Sci. **338**, 16 (2009)

Gervaso, F., Scalera, F., Padmanabhan, K., Sannino, A., Antonio Licciulli, A.: High-performance hydroxyapatite scaffolds for bone tissue engineering applications. Int. J. Appl. Ceram. Technol. **9**, 507–516 (2012)

Govindarajan, T., Shandas, R.: A survey of surface modification techniques for next-generation shape memory polymer stent devices. Polymers **6**, 2309–2331 (2014)
Janotti, A., Van de Walle, C.G.: Fundamentals of zinc oxide as a semiconductor. Rep. Prog. Phys. **72**, 126501 (2009)
Jiang, H., Liang, J., Grant, J.T., Su, W., Bunning, T.J., Cooper, T.M., Adams, W.W.: Characterization of chitosan and rare-earth-metal-ion doped chitosan films. Macromol. Chem. Phys. **198**, 1561 (1997)
Johnson, R., Hultqvist, A., Bent, S.: A brief review of atomic layer deposition: from fundamentals to applications. Mat. Tod. **17**, 236–246 (2014)
Kohal, R.J., Bachle, M., Att, W., Chaar, S., Altmann, B., Renz, A., et al.: Osteoblasts and bone tissue response to surface modified zirconia and titanium implant materials. Dent. Mater. **29**, 763–766 (2013)
Kostov, K.L., Belamie, E., Alonso, B., Mineva, T.: Surface chemical states of cellulose, chitin and chitosan studied by density functional theory and high-resolution photoelectron spectroscopy. Bulg Chem Commun **50**(Special Issue J), 135–146 (2018)
Laurenti, M., Cauda, V.: ZnO nanostructures for tissue engineering applications. Nanomaterials **7**, 374 (2017)
Li, J.Y., Chen, X.L., Li, H., He, M., Qiao, Z.Y.: Fabrication of zinc oxide nanorods. J. Cryst. Growth **233**, 5–7 (2001)
Li, C., Zang, Z., Han, C., Hu, Z., Tang, X., Du, J., Leng, Y., Sun, K.: Highly compact CsPbBr 3 perovskite thin films decorated by ZnO nanoparticles for enhanced random lasing. Nano Energy **40**, 195–202 (2017)
Laurenti, M., Stassi, S., Lorenzoni, M., Fontana, M., Canavese, G., Cauda, V., Pirri, C.F.: Evaluation of the piezoelectric properties and voltage generation of flexible zinc oxide thin films. Nanotechnology **26**, 215704 (2015)
Ma, P.X.: Biodegradable polymer scaffolds with well-defined interconnected spherical pore network. Tissue Eng. **7**, 23–33 (2001)
Martino, A.D., Sittinger, M., Risbud, M.V.: Chitosan: a versatile biopolymer for orthopaedic tissue-engineering. Biomaterials **26**, 5983–5990 (2005)
Milella, E., Cosentino, F., Licciulli, A., Massaro, C.: Preparation and characterization of titania/hydroxyapatite composite coatings obtained by sol-gel process. Biomaterials **22**, 1425–1431 (2001)
Mukherjee, S.: Laser Surface Modification of Ti_6Al_4V Implants. http://sciforum.net/conference/ecm-1, 1st International Electronics Conference on Materials (2014). Published: 30 May 2014
Muzzarelli, R.A.A.: Chitosan composites with inorganics, morphogenetic proteins and stem cells, for bone regeneration. Carbohydr. Polym. **83**, 1433–1445 (2011)
Narayan, R.J., Jin, C., Doraiswamy, A., Mihailescu, I.N., Jelinek, M., Ovsianikov, A., Chichkov, B., Chrisey, D.B.: Laser processing of advanced bioceramics. Adv. Eng. Mater. **9**, 83 (2007)
Narayan, R., Adiga, Sh, Pellin, M., Curtiss, L., Stafslien, S., Chisholm, B., Monteiro-Riviere, N., Brigmon, R., Elam, J.: Atomic layer deposition of nanoporous biomaterials. Mat. Today (2010). https://doi.org/10.1016/S1369-7021(10)70035-3
Nevins, M., Camelo, M., Nevins, M.L., Schupbach, P., Kim, D.M.: Pilot clinical and histologic evaluations of a two-piece zirconia implant. Int. J. Periodontics Restorative Dent. **31**, 157–163 (2011)
Olson, J., Atala, A., Yoo, J.: Tissue Engineering: current Strategies and Future Directions. Chonn. Med. J. **47**, 1–13 (2011)
Oviroh, P., Akbarzadeh, R., Pan, D., Coetzee, R., Jen, T.-C.: New development of atomic layer deposition: processes, methods and applications. Sci. Technol. Adv. Mat. **20**, 465–496 (2019)
Ozgur, U., Alivov, Y.I., Liu, C., Teke, A., Reshchikov, M.A., Dogan, S., Avrutin, V., Cho, S.J., Morkoc, H.: A comprehensive review of ZnO materials and devices. J. Appl. Phys. **98**, 041301 (2005)
Pighinelli, L., Guimarães, F., Paz, L., Zanin, G., Kmiec, M.: Calcium phosphate–chitosan and its derivatives biocomposities for hard tissue regeneration short review. Int. J. Clin. Chem. Lab. Med. **2**, 6–16 (2016)
Tosiriwatanapong, T., Singhatanadgit, W.: Zirconia-based biomaterials for hard tissue reconstruction. Bone Tissue Regen. Ins. **9**, 1–9 (2018)
Saito, T., Teraoka, K., Ota, K.: Arrayed three-dimensional structures designed to induce and maintain a cell pattern by a topographical effect on cell behavior. Mater. Sci. Eng. C **49**, 256–261 (2015)
Scheinpflug, J., Pfeiffenberger, M., Damerau, A., Schwarz, F., Textor, M., Lang, A., Schulze, F.: Journey into bone models: a review. Genes **9**, 247–283 (2018)
Soci, C., Zhang, A., Xiang, B., Dayeh, S.A., Aplin, D.P.R., Park, J., Bao, X.Y., Lo, Y.H., Wang, D.: ZnO nanowire UV photodetectors with high internal gain. Nano Lett. **7**, 1003–1009 (2007)
Terakawa, M.: Femtosecond laser processing of biodegradable polymers. Appl. Sci. **8**, 1123 (2018)
Wang, Z.L., Song, J.H.: Piezoelectric nanogenerators based on zinc oxide nanowire arrays. Science **312**, 242–246 (2006)

Wang, W., Yeung, K.W.K.: Bone grafts and biomaterials substitutes for bone defect repair: a review. Bioact. Mater. **2**, 224–247 (2017)

Wang, C.X., Yin, L.W., Zhang, L.Y., Xiang, D., Gao, R.: Metal oxide gas sensors: sensitivity and influencing factors. Sensors **10**, 2088–2106 (2010)

Wang, H., Cao, S., Yang, B., Li, H., Wang, M., Hu, X., Sun, K., Zang, Z.: NH_4Cl Modified ZnO for High-Performance $CsPbIBr_2$ Perovskite Solar Cells via Low Temperature Process. Solar RRL (2019). https://doi.org/10.1002/solr.201900363

Wua, S., Liu, X., Yeung, K., Liu, Ch., Yang, X.: Biomimetic porous scaffolds for bone tissue engineering. Mat. Sci. Eng. R **80**, 1–36 (2014)

Zang, Z.: Efficiency enhancement of ZnO/Cu_2O solar cells with well oriented and micrometer grain sized Cu_2O films. Appl. Phys. Lett. **112**, 042106 (2018)

Zang, Z., Zeng, X., Du, J., Wang, M., Tang, X.: Femtosecond laser direct writing of microholes on roughened ZnO for output power enhancement of InGaN light-emitting diodes. Opt. Lett. **41**(15), 3463 (2016)

Zhu, P., Weng, Z.Y., Li, X., Liu, X.M., Wu, S.L., Yeung, K.W.K., Wang, X.B., Cui, Z.D., Yang, X.J., Chu, P.K.: Biomedical applications of functionalized ZnO nanomaterials: from biosensors to bioimaging. Adv. Mater. Interfaces **3**, 1500494 (2016)